Measurement and modelling of non-contact atomic force microscope cantilever properties from ultra-high vacuum to normal pressure conditions

2011 Meas. Sci. Technol. 22 055501

(http://iopscience.iop.org/0957-0233/22/5/055501)

Meas. Sci. Technol. **22** (2011) 055501 (6pp) doi:10.1088/0957-0233/22/5/055501

Measurement and modelling of non-contact atomic force microscope cantilever properties from ultra-high vacuum to normal pressure conditions

Jannis Lübbe, Matthias Temmen, Holger Schnieder and Michael Reichling

Fachbereich Physik, Universität Osnabrück, Barbarastraße 7, 49076 Osnabrück, Germany

E-mail: reichling@uos.de

Received 17 December 2010, in final form 24 February 2011
Published 23 March 2011
Online at stacks.iop.org/MST/22/055501

Abstract
The resonance frequency and Q-factor of cantilevers typically used for non-contact atomic force microscopy (NC-AFM) are measured as a function of the ambient pressure varied from 10^{-8} mbar to normal pressure. The Q-factor is found to be almost constant up to a pressure in the range of 10^{-2}–10^{-1} mbar and then decreases by about three orders of magnitude when increasing the pressure further to normal pressure. The decrease in the resonance frequency measured over the same pressure range amounts to less than 1% where a significant change is observed in the range of 10–10^3 mbar. The pressure dependence of the effective Q-factor and resonance frequency is approximated by analytical models accounting for different processes in the molecular and viscous flow regimes. By introducing a heuristic approach for describing the pressure dependence in the transition regime, we are able to well approximate the cantilever properties over the entire pressure range.

Keywords: non-contact atomic force microscopy (NC-AFM), cantilever, resonance frequency, Q-factor, ambient pressure

(Some figures in this article are in colour only in the electronic version)

1. Introduction

Dynamic scanning force microscopy operated in the non-contact mode (NC-AFM) has long been a domain of measurements under conditions of the ultra-high vacuum as in most non-contact atomic force microscopy implementations, imaging is based on the detection of small frequency shifts in the oscillation of a high-Q cantilever [1]. Oscillating the cantilever in a gas of finite pressure, specifically normal pressure, or in a fluid reduces the Q-factor dramatically while its resonance frequency is only slightly shifted towards smaller values [2]. Due to the reduction in the Q-factor, the force gradient detection sensitivity is strongly diminished [3]. However, it has been shown that the detection sensitivity for NC-AFM imaging in air and liquids is high enough to allow for atomic resolution imaging provided that the opto-electronic detection system is optimized to achieve its technical limits [4–6]. The quality of NC-AFM images obtained in air can further be enhanced by applying advanced experimental techniques such as robust feedback loops [7], Q-control [8] or bimodal detection [9]. With optimized equipment, molecular resolution in air has been demonstrated [10] and the relevance of the Q-factor for such measurements has clearly been pointed out [11]. The effective Q-factor [12] of a cantilever oscillating in air has been investigated for a variety of cantilever geometries and pressure ranges [13–18] and it has been shown that it can be increased by optimizing the cantilever geometry [19, 20]. However, to obtain a high Q-factor for NC-AFM measurements in a controlled atmosphere, it may be more straightforward to reduce the ambient pressure and it is, therefore, of interest to determine the precise dependence of the Q-factor on the pressure of the ambient atmosphere.

In this contribution we investigate the Q-factor and the resonance frequency of cantilevers oscillating in a gas atmosphere where the ambient pressure is varied from 10^{-8} mbar to normal pressure. We compare our measurements to models predicting the Q-factor based on the intrinsic damping of the cantilever, mounting losses and pressure-dependent terms accounting for damping in the molecular flow and viscous regimes and develop expressions covering the entire pressure range. Similarly, we approximate the pressure dependence of the resonance frequency by available analytical models.

There are several mechanisms contributing to the damping of an oscillating cantilever that we have extensively discussed in a recent publication [12]. The reciprocal of the effective Q-factor $1/Q_{\text{eff}}$ describes the total damping which is determined by the intrinsic damping $1/Q_0$ of the cantilever, the damping $1/Q_{\text{mount}}$ of the cantilever fixation in the SFM system and the air damping $1/Q_{\text{air}}$ which needs to be considered when experiments are not performed under UHV conditions:

$$\frac{1}{Q_{\text{eff}}} = \frac{1}{Q_0} + \frac{1}{Q_{\text{mount}}} + \frac{1}{Q_{\text{air}}} \quad . \tag{1}$$

The pressure dependence of the Q-factor of silicon cantilevers has been investigated experimentally by Blom *et al* [13] and by Bianco *et al* [18] for certain ranges of the ambient pressure. It is possible to distinguish between pressure regimes that are dominated by different damping mechanisms, namely the molecular flow regime and the viscous flow regime [13]. To distinguish these regimes, we introduce the Knudsen number

$$Kn = \frac{\lambda}{w} \tag{2}$$

defined by the mean free path of the gas molecules λ and the width w of the gas layer in motion, which is the cantilever width in our case [16]. The mean free path of the gas molecules is given by

$$\lambda = \frac{1}{\sqrt{2}\pi d^2 n} \qquad \text{and} \qquad n = \frac{p}{k_B T} \tag{3}$$

with the number density n, the pressure p, the temperature T and the Boltzmann constant k_B. The molecule diameter is assumed to be $d = 3.7 \times 10^{-10}$ m [21]. The viscous flow regime is defined as $Kn < 0.01$, the free molecular flow regime as $Kn > 10$ while the range $10 > Kn > 0.01$ is referred to as the transition regime where molecular as well as viscous damping contributes [16]. For a typical cantilever width of 30 μm, Kn equals 10 at a pressure of $P = 0.23$ mbar, while Kn equals 0.01 at a pressure of $P = 230$ mbar. For the molecular region, the pressure-dependent Q-factor is calculated based on a model derived by Christian [18, 22]:

$$Q_{\text{molecular}} = \frac{\pi \rho t f_0}{2} \sqrt{\frac{\pi}{2}} \sqrt{\frac{RT}{M}} \frac{1}{p} \tag{4}$$

with the density ρ of the cantilever material, the thickness t and the resonance frequency f_0 of the cantilever, the mass of the gas molecules M and R being the gas constant. For the viscous damping regime the model of Hosaka *et al* is used, which assumes the cantilever to consist of a string of spheres moving in a fluid [23]:

$$Q_{\text{viscous}} = \frac{4\rho t w f_0}{6\eta + 3w\sqrt{\eta(M/RT)\pi f_0 p}} \tag{5}$$

with η being the dynamic viscosity of the gas.

The pressure-dependent resonance frequency $f_0^M(p)$ of a cantilever exposed to a medium such as air or water has been investigated in detail by Elmer *et al* [24]. We follow this approach assuming a master function that yields a frequency shift independent of the cantilever width[1]:

$$\begin{aligned} \frac{\Delta f}{f_0} &= \frac{f_0^M(p) - f_0}{f_0} \\ &= \left(\sqrt{1 + (l/t)(\rho_M/\rho)(\pi^2/12\alpha_1)}\right)^{-1} - 1 \end{aligned} \tag{6}$$

with $\alpha_1 = 1.8751$. The density ρ_M is calculated from the ideal gas law assuming nitrogen gas at a pressure p as the surrounding medium. This approach is an approximation considering the shift in resonance frequency due to the additional mass to be moved by the cantilever oscillating in a dense gas but does not take the viscosity of the medium into account. We apply this model to describe the pressure dependence of the shift in resonance frequency observed in our experiments.

2. Experimental details

The oscillation behaviour of cantilevers is investigated using a test setup that has been described in detail elsewhere [12]. In brief, cantilevers are mounted with a clamp fixation so that they can easily be removed for further use. The test setup is housed in a compact vacuum chamber equipped with a turbomolecular pump and an ion getter pump. A combined pirani/cold-cathode vacuum gauge (PKR 251, Pfeiffer Vacuum, Asslar, Germany) allows us to measure the pressure from normal to UHV conditions (accuracy 30%, reproducibility 5%). The pressure in the chamber can be controlled by backfilling with dry nitrogen gas using a metering valve. The turbomolecular pump is switched off while measuring.

To measure the Q-factor, we use a sine wave generator to excite a piezo ceramic plate with gold electrodes glued to the cantilever holder and sweep the frequency in a range centred on the resonance frequency f_0 of the cantilever. A lock-in detector records the deflection signal as a function of the excitation frequency. The eigenfrequency f_0 and the Q-factor are obtained from the frequency spectrum taken under UHV conditions by a least-squares fit of the following equation to the data:

$$|A| = \frac{|A_{\text{exc}}|}{\sqrt{\left(1 - f_{\text{exc}}^2/f_0^2\right)^2 + f_{\text{exc}}^2/\left(f_0^2 Q^2\right)}} \tag{7}$$

[1] As suggested by Elmer *et al* [24], we use $\tilde{f}(\kappa) = \pi^2/(48\kappa)$ for the master function with $\kappa = \alpha_1 w/l$ and $\alpha_1 = 1.8751$ for oscillation at the fundamental resonance frequency of the cantilever. This yields surprisingly good agreement for the pressure-dependent frequency shift between theory and experiment. The agreement is much worse when using values for the master function numerically evaluated in the range of $\kappa = 0.2$–0.5 that is relevant for the investigated cantilevers.

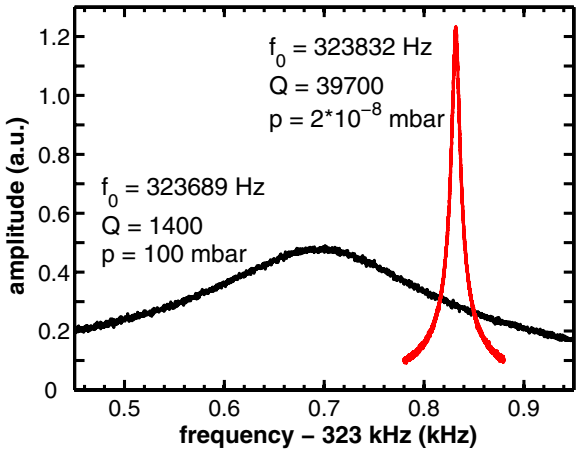

Figure 1. Resonance curves of a 300 kHz cantilever taken at a pressure of 2×10^{-8} mbar (narrow resonance) and 100 mbar (broad resonance).

where the cantilever is assumed to be a damped harmonic oscillator excited at the frequency f_{exc} with the amplitude A_{exc} [25]. This equation is valid for $Q \gg 1$ which is usually fulfilled in air and vacuum. Only for very low-Q environments, such as water where Q is in the order of 1, do dissipative effects of the fluid need to be considered, yielding a different response function [27]. For this measurement it is important to adjust the sweep speed to the time constants involved in the measurement. For high-Q 75 kHz cantilevers, the amplitude time constant $\tau_Q = Q/(\pi f_0)$ is typically 0.7 s under UHV conditions defining the upper limit [26]. The time constant of the lock-in detector recording the cantilever oscillation signal is set to $\tau_{\mathrm{LI}} = 0.3$ s while the sweep time is typically $t_{\mathrm{sweep}} = 200$ s. For a precision measurement of Q, the sweep range is chosen to be symmetric about the resonance frequency with start and stop set to frequencies where the oscillation amplitude is about 0.1 times the on-resonance maximum. By this adjustment, any distortion of the recorded resonance curve and corruption of the determined Q-factor resulting from an inappropriate choice of the effective measurement time constant and the sweep speed can be excluded.

3. Results and discussion

In the first set of experiments, we measure the Q-factor and resonance frequency and compare results obtained under UHV conditions to those obtained at normal pressure or slightly below. Increasing the pressure by ten orders of magnitude starting from UHV conditions results in a slight shift in the resonance frequency but a dramatic reduction in the Q-factor as demonstrated by the example resonance curves shown in figure 1. This figure shows a narrow resonance curve of a 300 kHz cantilever recorded under UHV conditions and a broad resonance curve of the same cantilever recorded after backfilling the chamber to a pressure of 100 mbar. In table 1, the quality factors $Q_{\mathrm{eff}}^{\mathrm{air}}$ of different cantilevers measured at normal pressure are compared to the corresponding values $Q_{\mathrm{eff}}^{\mathrm{vac}}$ obtained in UHV. A major conclusion to be drawn from this table is that there is no correlation of Q-factors measured in air with the respective UHV values. Even within a group of the same type of cantilevers, the order of increasing Q-factors in air does not correspond to the values in UHV, which is most obvious for the cantilevers in the 60 kHz range. Therefore, it is not possible to obtain any estimate for a Q-factor effective in UHV from a measurement performed in air.

Table 1. Q-factors $Q_{\mathrm{eff}}^{\mathrm{vac}}$ and resonance frequencies f_0 of cantilevers representative of two different types measured in UHV compared to values $Q_{\mathrm{eff}}^{\mathrm{air}}$ and f_0^{air} measured in air. $Q_{\mathrm{eff}}^{\mathrm{vac}}$ is determined at a pressure in the range of 10^{-7}–10^{-8} mbar and $Q_{\mathrm{eff}}^{\mathrm{air}}$ is measured at normal pressure.

$Q_{\mathrm{eff}}^{\mathrm{air}}$	$Q_{\mathrm{eff}}^{\mathrm{vac}}$	f_0^{air} (Hz)	f_0 (Hz)
220	95 700	61 182	61 437
340	65 400	64 830	64 788
360	133 700	63 210	63 562
420	31 500	315 128	316 004
450	35 300	291 841	294 108
460	12 900	301 926	302 704
660	11 900	291 378	291 809
690	7 700	297 108	297 675
1160	38 500	320 862	323 804

Next, we investigate in detail the pressure dependence of the Q-factor and the resonance frequency of four silicon cantilevers manufactured by Nanoworld AG (Neuchâtel, Switzerland) that are typically used for NC-AFM measurements, namely cantilever 1 (type FM, $f_0 \approx 60$ kHz), cantilever 2 (type NCH, $f_0 \approx 300$ kHz), cantilever 3 (type NCL, $f_0 \approx 170$ kHz) and cantilever 4 (special development probe L250T10, $f_0 \approx 190$ kHz). The key parameters of these cantilevers are compiled in table 2. Cantilevers 1, 3 and 4 are of similar length, 3 and 4 have similar resonance frequencies but all cantilevers differ from each other significantly in thickness. In table 2, the resonance frequency f_0 measured in UHV is compared to $f_0^{\mathrm{air,exp}}$ measured under ambient pressure conditions and a theoretical value $f_0^{\mathrm{air,theo}}$ calculated using equation (6). The theoretical resonance frequency in UHV is not mentioned here because an accurate calculation requires precise knowledge of the tip mass. Figure 2 shows the normalized shift $\Delta f/f_0$ of the resonance frequency as a function of pressure p compared to theory. As evident from equation (6), the pressure-dependent shift of the resonance frequency depends on the ratio of length and thickness of the cantilever. For the dimensions of cantilever 1, this ratio is about three times larger than for the other cantilevers explaining the higher sensitivity of the resonance frequency to air damping.

Using the known material properties of silicon cantilevers and the dimensions of the cantilevers investigated here (see table 2), we calculate Q_0^{theo} according to a procedure described in detail in [12] and compile results in table 3. The discrepancy between Q_0^{theo} and the effective value Q_{eff} is explained by the mounting loss Q_{mount}. For cantilevers 2 and 4, the measured effective Q-factor is slightly larger than the theoretical value which is due to errors in determining cantilever dimensions. Practically this means that there is a negligible mounting loss ($Q_{\mathrm{mount}} = \infty$). Finally, the measured effective Q-factors in air are compared to calculated values at 10^3 mbar. From

Table 2. Dimensions, length l, width w and thickness t (see [12]), of the four investigated cantilevers related to their resonance frequency as calculated or measured. The resonance frequency $f_0^{\text{air,exp}}$ in air measured under ambient conditions is compared to a theoretical value $f_0^{\text{air,theo}}$ calculated using equation (6) using the resonance frequency f_0 measured under UHV conditions.

Cantilever	l (μm)	w (μm)	t (μm)	f_0 (Hz)	$f_0^{\text{air,theo}}$ (Hz)	$f_0^{\text{air,exp}}$ (Hz)
1	227	27	2.6	61 758	61 196	61 341
2	125	34	4.1	302 200	301 230	301 330
3	228	39	7.3	170 410	169 850	170 070
4	253	72	9.6	191 020	190 490	190 530

Dimensions of the cantilevers have been determined by the manufacturer using an optical microscope (length l and width w) and a laser interferometer (thickness t). The accuracy is $\Delta l = \pm 2.5\,\mu$m, $\Delta w = \pm 1.5\,\mu$m and $\Delta t = \pm 0.2\,\mu$m, respectively.

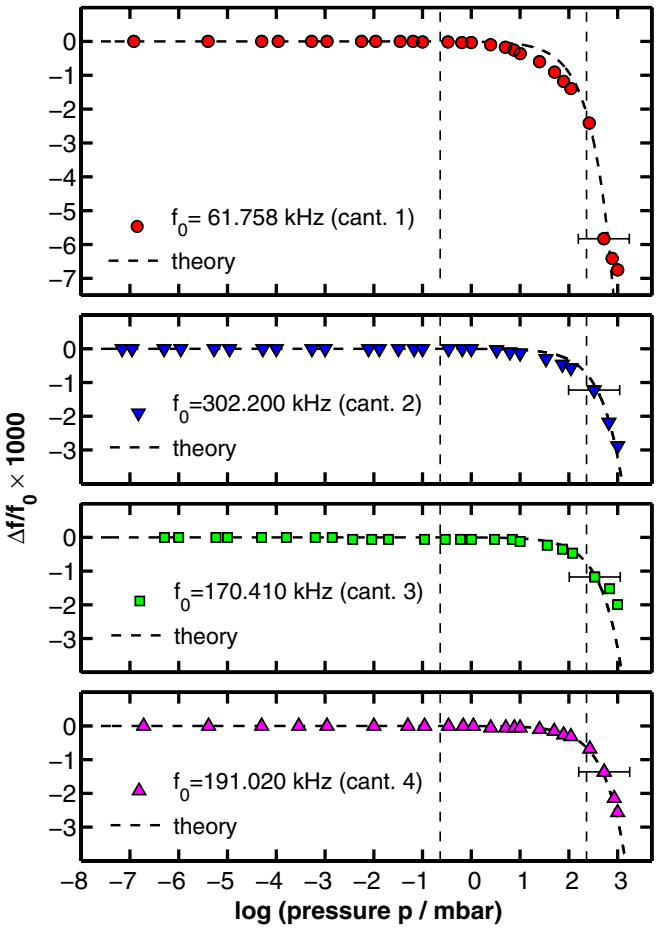

Figure 2. Relative shift $\Delta f/f_0$ of the resonance frequency of the four investigated cantilevers with different dimensions as a function of the ambient pressure. Starting at UHV conditions, the vacuum chamber is back filled with nitrogen gas until normal pressure is reached.

Table 3. Q-factors Q_0^{theo} of the four investigated cantilevers calculated from the models described in [12] and cantilever properties given in table 2. The error of Q_0^{theo} resulting from the error of dimensional measurements is 11% for cantilever 1, 19% for cantilever 2, 9% for cantilever 3 and 7% for cantilever 4. Q_{eff} are the measured effective Q-factors with the corresponding calculated values of Q_{mount}. The effective Q-factor $Q_{\text{eff}}^{\text{air,exp}}$ in air measured under ambient conditions is compared to a theoretical value $Q_{\text{eff}}^{\text{air,theo}}$ calculated using equation (1).

Cantilever	Q_0^{theo}	Q_{eff}	Q_{mount}	$Q_{\text{eff}}^{\text{air,theo}}$	$Q_{\text{eff}}^{\text{air,exp}}$
1	458 700	182 400	302 900	160	300
2	40 400	43 900	∞	730	640
3	34 500	26 500	114 300	930	870
4	19 500	21 700	∞	1390	810

this table, it can clearly be seen that the damping due to the ambient gas by orders of magnitude exceeds any other effect and, therefore, Q_{air} is clearly the dominating contribution to the effective Q-factor. Figure 3(a) shows a measurement of the Q-factor of cantilever 1 as a function of pressure together with model predictions for this cantilever. The dash-dotted line describes the measured effective Q-factor (UHV value) combined with a calculation of the viscous damping according to equation (5). The dotted line describes the combination of the effective Q-factor with a calculation for the molecular damping according to equation (4). As $Q_{\text{molecular}}$ vanishes for high pressure and Q_{viscous} becomes negligible for low pressure compared to the contribution of $Q_{\text{molecular}}$, we approximate $Q_{\text{air}} = Q_{\text{molecular}} + Q_{\text{viscous}}$ to yield an expression for the transition pressure range which is shown by the solid line. The heuristic approach of adding Q-factors is physically not correct but practically generates a curve that describes the experimental data very well over the entire pressure range from UHV to normal conditions. Furthermore, the pressure dependence of the calculated intrinsic Q_0 is shown as a dashed line. This curve is directly based on known dimensional properties of the cantilever without any fitting or Q-factor measurement. The difference between Q_0 and Q_{eff} stems from the contribution of Q_{mount} as described in detail in [12]. By including mounting losses, we are able to describe the pressure dependence rather precisely and transfer this methodology to the description of other cantilevers.

Figure 3(b) shows the Q-factors of the four investigated cantilevers as a function of the ambient pressure. Up to a pressure of 10^{-4} mbar, the measured Q-factors remain virtually unchanged compared to UHV conditions. In this region, no viscous damping occurs but collisions of the cantilever with the increasing number of residual gas molecules result in a slight reduction of the Q-factor. A dramatic reduction of Q is observed for pressures above 10^{-2} mbar for cantilever 1 and above 10^{-1} mbar for the other cantilevers. This can be understood as $Q_{\text{molecular}}$ is governed by the factor $t \times f_0$

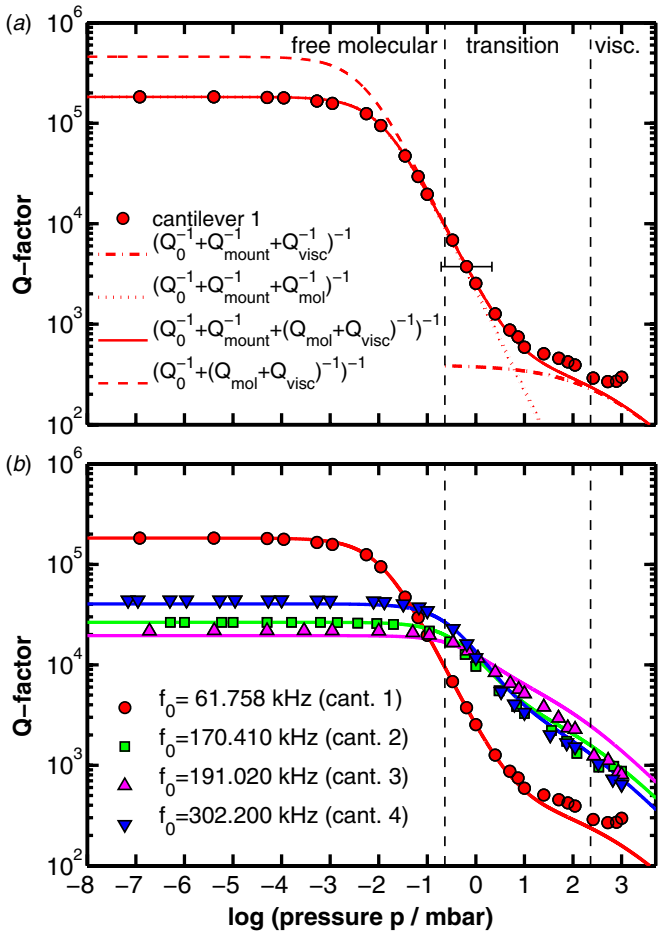

Figure 3. (*a*) Measurement of the effective Q-factor of cantilever 1 as a function of pressure. Starting at UHV conditions, the test chamber is back filled with nitrogen until ambient pressure is reached. The plots show the measured Q_{eff} combined with the air damping in the viscous regime (dash-dotted line), the air damping in the molecular regime (dotted line) and the sum $Q_{\mathrm{mol}} + Q_{\mathrm{visc}}$ (solid line). Additionally, measurements are compared to the calculated intrinsic value Q_0 combined with the sum $Q_{\mathrm{mol}} + Q_{\mathrm{visc}}$ (dashed line). The discrepancy between the intrinsic and the effective Q-values is explained by Q_{mount} (see table 3). (*b*) Measured effective Q-factor of the four investigated cantilevers as a function of ambient pressure. For cantilever 4, the borders of molecular and viscous regimes should be shifted to higher pressure by a factor of 2 because of the significantly larger cantilever width. In the logarithmic plot, this is, however, a minor correction that has been omitted for simplicity of the figure.

which is about ten times smaller for cantilever 1 than for the other cantilevers. When the pressure approaches normal conditions, Q_{eff} is completely controlled by Q_{air} for all types of investigated cantilevers and we find good agreement in both the free molecular flow and viscous flow regimes. In the transition regime, however, neither model can well describe the pressure dependence of the Q-factor and we use the described heuristic approach to interpolate.

In summary, we measure the Q-factor of four different types of NC-AFM cantilevers differing in geometry over a range of 11 decades of ambient pressure. For all types of cantilevers, the pressure dependence can well be described by theoretical models based on the physics of free molecular flow and viscous flow while we can well interpolate in the transition regime. This result is of practical use for measurements performed at elevated pressure as the methodology introduced here allows a prediction of the Q-factor enhancement when reducing the ambient pressure from normal pressure to a value lower by up to five orders of magnitude based on a knowledge of cantilever dimensions only. Our results, furthermore, highlight the different physical origins of the pressure-dependent shift in resonance frequency and the Q-factor of the cantilever. The shift in resonance frequency can solely be described considering the mass added by the surrounding medium for a cantilever oscillating in a gas of sufficient density and does not significantly depend on the viscosity of the gas for the investigated pressure range. The pressure dependence of the Q-factor, on the other hand, is solely governed by molecular impact for lower pressures and by viscosity for higher pressures. Consequently, the ambient gas pressure provides a convenient means of tuning the Q-factor of an oscillating cantilever over a wide range without strongly changing the resonance frequency similar to the recently demonstrated tuning of the Q-factor by opto-thermal pressure exerted on a cantilever in an optical cavity [2].

Acknowledgments

We are grateful to Christoph Richter (Nanoworld Services GmbH, Germany) for continued interest in this work and support of the measurements. Support from the Deutsche Forschungsgemeinschaft via the Graduiertenkolleg 695 is gratefully acknowledged.

References

[1] Morita S, Wiesendanger R and Meyer E 2002 Noncontact atomic force microscopy *NanoScience and Technology* (Berlin: Springer)

[2] Tröger L and Reichling M 2010 Quantification of antagonistic optomechanical forces in an interferometric detection system for dynamic force microscopy *Appl. Phys. Lett.* **97** 213105

[3] Albrecht T R, Grütter P, Horne D and Rugar D 1991 Frequency modulation detection using high-Q cantilevers for enhanced force microscopy sensitivity *J. Appl. Phys.* **69** 668–73

[4] Fukuma T, Kimura M, Kobayashi K, Matsushige K and Yamada H 2005 Development of low noise cantilever deflection sensor for multienvironment frequency-modulation atomic force microscopy *Rev. Sci. Instrum.* **76** 053704

[5] Fukuma T and Jarvis S P 2006 Development of liquid-environment frequency modulation atomic force microscope with low noise deflection sensor for cantilevers of various dimensions *Rev. Sci. Instrum.* **77** 043701

[6] Suzuki K, Kitamura S, Tanaka S, Kobayashi K and Yamada H 2010 Development of high-resolution imaging of solid–liquid interface by frequency modulation atomic force microscopy *Japan. J. Appl. Phys.* **49** 08LB12

[7] Kilpatrick J I, Gannepalli A, Cleveland J P and Jarvis S P 2009 Frequency modulation atomic force microscopy in ambient environments utilizing robust feedback tuning *Rev. Sci. Instrum.* **80** 023701

[8] Hölscher H, Ebeling D and Schwarz U D 2006 Theory of *Q*-controlled dynamic force microscopy in air *J. Appl. Phys.* **99** 084311
[9] Martínez N F, Lozano J R, Herruzo E T, Garcia F, Richter C, Sulzbach T and Garcia R 2008 Bimodal atomic force microscopy imaging of isolated antibodies in air and liquids *Nanotechnology* **19** 384011
[10] Farrell A A, Fukuma T, Uchihashi T, Kay E R, Bottari G, Leigh D A, Yamada H and Jarvis S P 2005 Conservative and dissipative force imaging of switchable rotaxanes with frequency-modulation atomic force microscopy *Phys. Rev.* B **72** 125430
[11] Fukuma T, Ichii T, Kobayashi K, Yamada H and Matsushige K 2005 True-molecular resolution imaging by frequency modulation atomic force microscopy in various environments *Appl. Phys. Lett.* **86** 034103
[12] Lübbe J, Tröger L, Bechstein R, Richter C, Kühnle A and Reichling M 2010 Achieving high effective *Q*-factors in ultra-high vacuum dynamic force microscopy *Meas. Sci. Technol.* **21** 125501
[13] Blom F R, Bouwstra S, Elwenspoek M and Fluitman J H J 1992 Dependence of the quality factor of micromachined silicon beam resonators on pressure and geometry *J. Vac. Sci. Technol.* B **10** 19–26
[14] Lévêque G, Girard P, Belaidi S and Solal G C 1997 Effects of air damping in noncontact resonant force microscopy *Rev. Sci. Instrum.* **68** 4137–44
[15] Li B, Wu H, Zhu C and Liu J 1999 The theoretical analysis on damping characteristics of resonant microbeam in vacuum *Sensors Actuators* **77** 191–4
[16] Mertens J, Finot E, Thundat T, Fabre A, Nadal M H, Eyraud V and Bourillot E 2003 Effects of temperature and pressure on microcantilever resonance response *Ultramicroscopy* **97** 119–26
[17] Suzuki Y, Enoki H and Akiba E 2004 Investigation of influence of gas atmosphere and pressure upon non-contact atomic force microscopy *Ultramicroscopy* **99** 221–6
[18] Bianco S *et al* 2006 Silicon resonant microcantilevers for absolute pressure measurement *J. Vac. Sci. Technol.* B **24** 1803–9
[19] Lee J H, Lee S T, Yao C M and Fang W L 2007 Comments on the size effect on the microcantilever quality factor in free air space *J. Micromech. Microeng.* **17** 139–46
[20] Naeli K and Brand O 2009 Dimensional considerations in achieving large quality factors for resonant silicon cantilevers in air *J. Appl. Phys.* **105** 014908
[21] Pandey A K, Pratap R and Chau F S 2007 Effect of pressure on fluid damping in MEMS torsional resonators with flow ranging from continuum to molecular regime *Exp. Mech.* **48** 91–106
[22] Christian R G 1966 The theory of oscillating-vane vacuum gauges *Vacuum* **16** 175–8
[23] Hosaka H, Itao K and Kuroda S 1995 Damping characteristics of beam-shaped micro-oscillators *Sensors Actuators* A **49** 87–95
[24] Elmer F J and Dreier M 1997 Eigenfrequencies of a rectangular atomic force microscope cantilever in a medium *J. Appl. Phys.* **81** 7709–14
[25] Giessibl F J 2003 Advances in atomic force microscopy *Rev. Mod. Phys.* **75** 949–83
[26] Stipe B C, Mamin H J, Stowe T D, Kenny T W and Rugar D 2001 Noncontact friction and force fluctuations between closely spaced bodies *Phys. Rev. Lett.* **87** 096801
[27] Sader J E 1998 Frequency response of cantilever beams immersed in viscous fluids with applications to the atomic force microscope *J. Appl. Phys.* **84** 64–76